Absence of Topological Protection of the Interface States in $\mathbb{Z}_2$ Photonic Crystals

Shupeng Xu,[†] Yuhui Wang,[†] and Ritesh Agarwal[*]
Department of Materials Science and Engineering, University of Pennsylvania, Philadelphia, Pennsylvania 19104, USA

(Received 26 December 2022; accepted 13 July 2023; published 1 August 2023)

Inspired from electronic systems, topological photonics aims to engineer new optical devices with robust properties. In many cases, the ideas from topological phases protected by internal symmetries in fermionic systems are extended to those protected by crystalline symmetries. One such popular photonic crystal model was proposed by Wu and Hu in 2015 for realizing a bosonic $\mathbb{Z}_2$ topological crystalline insulator with robust topological edge states, which led to intense theoretical and experimental studies. However, a rigorous relationship between the bulk topology and edge properties for this model, which is central to evaluating its advantage over traditional photonic designs, has never been established. In this Letter, we revisit the expanded and shrunken honeycomb lattice structures proposed by Wu and Hu and show that they are topologically trivial in the sense that symmetric, localized Wannier functions can be constructed. We show that the $\mathbb{Z}$ and $\mathbb{Z}_2$ type classifications of the Wu-Hu model are equivalent to the C_2T protected Euler class and the second Stiefel-Whitney class, respectively, with the latter characterizing the full valence bands of the Wu-Hu model, indicating only a higher order topological insulator. Additionally, we show that the Wu-Hu interface states can be gapped by a uniform topology preserving C_6 and T symmetric perturbation, which demonstrates the trivial nature of the interface. Our result reveals that topology is not a necessary condition for the reported helical edge states in many photonics systems and opens new possibilities for interface engineering that may not be constrained by topological considerations.

DOI: 10.1103/PhysRevLett.131.053802

Topological photonics began with the seminal work by Raghu and Haldane [1,2] where the idea of topology in the electronic band structures were generalized to waves in periodic media, leading the way for realizing topological phenomena in artificial structures [3–5]. The early explorations of topological photonics were focused on the photonic Chern insulators where the time-reversal symmetry is explicitly broken [6,7]. With the discovery of topological crystalline insulators (TCIs) [8], the topological phases were significantly enriched beyond the tenfold way classification of topological insulators and superconductors [9] that opened new opportunities in engineering topological phases in bosonic systems.

However, one has to be cautious when generalizing the ideas from the early examples of topological phases, especially to those that are protected by crystalline symmetries. For example, due to the fact that crystalline symmetry is often broken at a physical boundary, some TCIs only exhibit robust boundary states at certain crystal orientations [8]. Moreover, with the discovery of novel states such as fragile topological phases [10–13] and higher order topological insulators [14,15], the notion of bulk-boundary correspondence of codimension 1 may not have any direct generalization to TCIs at all.

The topological photonic crystal proposed by Wu and Hu [16], which we refer to as the Wu-Hu model, is an elegant structure for realizing a proposed bosonic analog of the fermionic $\mathbb{Z}_2$ topological insulator (TI) (Fig. 1). Hence it is claimed to host symmetry protected edge states that enable robust light transport free from backscattering. The simplicity of the model triggered innumerous experimental and theoretical studies after its discovery [17–37]. However, the exact bulk-boundary correspondence has never been identified; therefore, the robustness of the edge states and their relation to the bulk topology remain unclear. Here, we revisit the Wu-Hu model and analyze the nature of its topology with a special emphasis on the edge properties.

We briefly review the original formalism of the Wu-Hu model as the foundation of discussion. The tight-binding model of an expanded or shrunken honeycomb lattice provides a faithful description of the Wu-Hu model in which the unit cell for a graphene lattice is enlarged to include six atomic sites, and the couplings are divided into intracell (t_1) and intercell (t_2) couplings [Fig. 1(a)]. When $t_1 = t_2$, a fourfold degeneracy appears at the Γ point, which gives rise to a "double Dirac cone." The cell-periodic part of the degenerate Bloch functions have the symmetries of $|p_\pm\rangle$ and $|d_\pm\rangle$ orbitals, and a gap opening and band inversion can be achieved by tuning the relative magnitudes of t_1 and t_2 [Figs. 1(c) and 1(e)].

At certain high symmetry momenta, a composite pseudofermionic time-reversal symmetry $\tilde{\mathcal{T}}^2 = -1$ was constructed and the $\mathbb{Z}_2$ topology was derived through the analogy to the spinful case. For example, at the Γ point in

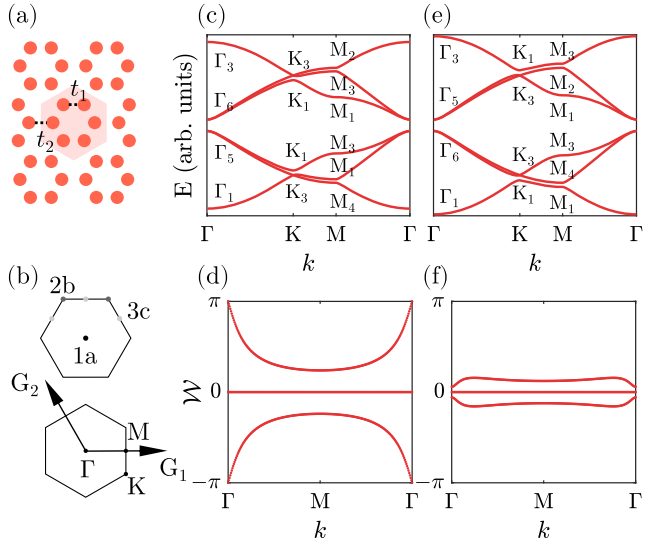

FIG. 1. (a) A schematic of the Wu-Hu lattice. The shadowed area indicates the hexagonal unit cell; t_1 (t_2) correspond to intracell (intercell) couplings. When each site moves away from (toward) the unit cell center, $t_1 < t_2$ ($t_1 > t_2$), it is referred to as an expanded (shrunken) phase. (b) (top) $1a$, $2b$, $3c$ Wyckoff positions of the unit cell color coded in black, dark gray, and light gray, located at the center, vertices, and edges, respectively; (bottom) Brillouin zone of a triangular lattice. (c),(d) The band structure of an expanded phase and its corresponding Wilson loop. (e),(f) The band structure of a shrunken phase and its corresponding Wilson loop. Irreps are noted in the band diagrams at each high symmetry point. Note in (c) and (e), Γ_5 and Γ_6 are representations of d and p orbital states, respectively, therefore showing the band inversion. In (d) and (f), both phases show trivial Wilson loop without winding from $-\pi$ to π.

the $(|p_x\rangle, |p_y\rangle)$ basis, the pseudo time-reversal operator is given by

$$\tilde{\mathcal{T}} = \mathcal{U}\mathcal{K} = [D_{E_1}(C_6) + D_{E_1}(C_6^2)]/\sqrt{3}\,\mathcal{K} = -i\sigma_y\mathcal{K}, \qquad (1)$$

in which E_1 is the irreducible representation (irrep) for $6mm1'$ (the little cogroup at Γ) furnished by $(|p_x\rangle, |p_y\rangle)$ orbitals and $D_{E_1}(C_6)$ is the corresponding matrix representation of C_6; $\mathcal{K}$ is the bosonic time-reversal operator. Equation (1) satisfies $\tilde{\mathcal{T}}^2 = -1$ and thus protects Kramer's degeneracy at Γ point.

The $\mathbb{Z}_2$ index was obtained through the parity of spin-Chern number for each pseudospin channel where the $|p_+\rangle(|p_-\rangle)$ and $|d_+\rangle(|d_-\rangle)$ orbitals are assigned with pseudospin up (down) [16,32]. The bulk-boundary correspondence of the 2D spinful TI was directly applied in the original proposal. The interface states between different phases of Wu-Hu model were claimed to be gapless (with a tiny gap due to the C_6 breaking at the interface), immune from backscattering and possess spin-momentum locking.

It is, however, not fully justified why Eq. (1) would constrain the global algebraic classification of Bloch functions and imply physical consequences exactly the same as the time-reversal symmetry in spinful systems. Here, we examine the topology of the Wu-Hu model using topological quantum chemistry [38–42] and Wilson loop methods [12,43,44], which are two important tools to diagnose nontrivial topology with Wannier obstruction when crystalline symmetry is involved. The Wannier obstruction is important because it can be directly related to the topological boundary states [45,46]. It has been recently shown that for continuum experimental systems the Wannier obstruction is a necessary condition for robust interface states [47], which is of utmost importance.

In topological quantum chemistry, the symmetry properties of the Bloch functions of Wannier-representable bands is equivalent to a direct sum of elementary band representations (EBRs). Throughout the Brillouin zone, the symmetry properties can be well described by the collection of irreducible representations (irreps) furnished by the Bloch functions for the little groups at high symmetry momenta. In Figs. 1(c) and 1(e), we calculate the irreps at high symmetry momenta for both shrunken and expanded phases in the Wu-Hu model and the relevant EBRs are listed in Table I [48–51]. For the valence bands (VBs), we obtain $(A_1{\uparrow}G)_{1a} \oplus (E_1{\uparrow}G)_{1a}$ for the shrunken case and $(A_1{\uparrow}G)_{3c}$ for the expanded case, respectively. The VBs for both phases transform as a direct sum of EBRs, which suggests the trivial nature of the bulk topology.

We also calculated the phase of the eigenvalues of the Wilson loop operator, which is defined by the following path ordered integral [43]:

$$\mathcal{W}_C = \mathcal{P}\exp\left[i\oint_C \boldsymbol{A}(\boldsymbol{k})\cdot d\boldsymbol{k}\right], \qquad (2)$$

where $[\boldsymbol{A}(\boldsymbol{k})]_{mn} = i\langle u_m(\boldsymbol{k})|\nabla_{\boldsymbol{k}}|u_n(\boldsymbol{k})\rangle$ is the non-Abelian Berry connection for the full VBs. Figure 1(b) shows the geometry of the Wilson loop, where the closed loop C is defined by the reciprocal lattice vector G_1 and the spectra is plotted as the loop moves along G_2 [Figs. 1(d) and 1(f)]. For both phases of the Wu-Hu model, no winding is observed, which also suggests that the whole VBs can be smoothly deformed into a trivial atomic insulator.

Next, we briefly discuss the topological invariants for the VBs of the Wu-Hu model. In the Supplemental Material [52] we prove that the spin-Chern number and the $\mathbb{Z}_2$ index

TABLE I. The EBRs for space group $P6mm1'$ (the symmetry of the Wu-Hu model). The EBRs are induced representations of localized orbitals and are labeled by $(\rho{\uparrow}G)_p$ in which p is the Wyckoff position where the orbitals sit, ρ is the irrep furnished by the orbitals, and G is the space group of the system.

Band representations	$(A_1{\uparrow}G)_{1a}$	$(E_1{\uparrow}G)_{1a}$	$(A_1{\uparrow}G)_{3c}$
Γ	Γ_1	Γ_6	$\Gamma_1 \oplus \Gamma_5$
K	K_1	K_3	$K_1 \oplus K_3$
M	M_1	$M_3 \oplus M_4$	$M_1 \oplus M_3 \oplus M_4$

defined for Wu-Hu model are equivalent to the Euler class and the second Stiefel-Whitney class protected by $C_2\mathcal{T}$ symmetry [13,54–59]. In 2D systems with $C_2\mathcal{T}$ symmetry, two-band subspaces are classified by the $\mathbb{Z}$ type Euler class. A nonzero Euler class forbids the construction of symmetric localized Wannier functions; however, this obstruction may be lifted by adding trivial bands. In this many-band limit, the parity of the Euler class becomes the well defined $\mathbb{Z}_2$ type second Stiefel-Whitney class ω_2. The expanded phase belongs to this category and is characterized by a nontrivial $\omega_2 = 1$, which indicates that the Wannier functions cannot be localized at the center of the unit cell. The associated physical consequence is a quantized quadrupole moment and fractional corner charges; in other words, $\omega_2 = 1$ characterizes a higher order topological insulator [35,36,54,58–60].

In fact, it can be shown that the VBs for both phases of Wu-Hu model are adiabatically connected to decoupled atomic clusters by selectively turning off intracell or intercell couplings (referred to as "strong binding limit"), which agrees well with the above analysis. With all these observations we conclude that both phases of the Wu-Hu model are topologically trivial in terms of Wannier obstruction; therefore, neither of the two phases are responsible for the gapless interface states. This can be demonstrated in the tight-binding calculation. Starting with the gapless interface and adiabatically turning off the couplings connecting two phases to form two open boundary conditions (OBCs), the edge states would be in general gapped and pushed toward the bulk bands. If the interface or edge states are results from the nontrivial bulk topology, we can keep track of them and they should be localized exactly at the nontrivial half of the system. However, depending on the edge configuration, the edge states can be localized at different phases. The edge inevitably breaks the integrity of at least one type of the decoupled clusters in the strong binding limit, which is referred as "cutting" through the corresponding Wannier center in the following context. In Fig. 2, we show that for the shrunken phase where the Wannier center sits at $1a$ Wyckoff position, the gapped edge states appear when the boundary cuts through $1a$ position; for the expanded case where the Wannier center sits at $3c$ Wyckoff position, the gapped edge states appear when the edge cuts through $3c$ Wyckoff position. This observation strongly suggests that the interface states are originated from the local defects in contrast to the well-known topological boundary states arising from the bulk Wannier obstruction [45,46].

Typically, the interface states are explained by the direct generalization of the bulk-boundary correspondence of the 2D spinful TI. However, the Kramer's degeneracy in 1D Brillouin zone cannot be protected by the composite pseudofermionic time-reversal operator in the Wu-Hu model, thus invalidating the generalization. An alternate

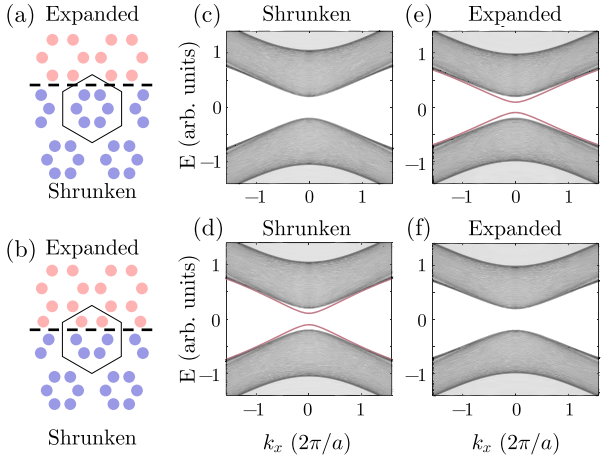

FIG. 2. (a),(b) Demonstration of two distinct edge configurations. Red (blue) sites correspond to the expanded (shrunken) phase, and a complete hexagonal unit cell is marked in the figure. In (a), the edge cuts through $3c$ Wyckoff position whereas in (b) through $1a$ Wyckoff position. The hopping across the cut is zero so that the expanded and shrunken regions are decoupled and the dispersion is calculated individually for each region. (c), (e) Energy dispersion in a strip geometry with edge configuration shown in (a). The gapped edge states only show up in the expanded phase. (d),(f) Energy dispersion with edge configuration shown in (b). The gapped edge states only show up in the shrunken phase.

interpretation explains the interface states as the Jackiw-Rebbi soliton eigen solutions that arise from a local band inversion [32]. However, since the Jackiw-Rebbi solutions give one set of interface states for each pseudospin, spin mixing can potentially gap out the interface states. And the symmetry that protects the bulk topology in the Wu-Hu model, namely C_6 and $\mathcal{T}^2 = 1$, does not imply spin conservation. Consider the Wu-Hu model in its quasiorbital basis, where $|p_\pm\rangle$ and $|d_\pm\rangle$ orbitals sit at $1a$ Wyckoff position of a triangular lattice. The spin flipping terms are locally forbidden by C_6 symmetry, but the following nonlocal spin-flip channel is always allowed:

$$\Delta = t a^\dagger_{i,\pm} a_{j,\mp} + \text{H.c.}, \qquad i \neq j, \tag{3}$$

where i, j are labels of unit cells and $\pm$ are labels for pseudospins and H.c. stands for Hermitian conjugate.

Here, we explicitly show that the interface states can be gapped considerably even by a C_6 and $\mathcal{T}^2 = 1$ symmetric perturbation that is uniform across the interface (Fig. 3). The perturbation is added to ensure that when $t_1 = t_2$, a double Dirac cone appears at Γ point. The band inversion is then achieved by tuning the relative magnitude of t_1 and t_2 (see Supplemental Material [52]). Therefore, the original Wu-Hu Hamiltonian is explicitly included. Also, no gap closing ever happened between the VBs and conduction bands under the perturbation; thus, the topology is

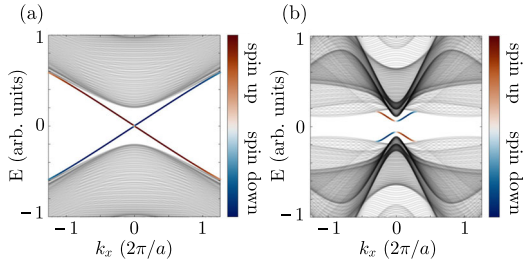

FIG. 3. The dispersion of interface states where the pseudospin component is color coded. (a) The interface states of an unperturbed Wu-Hu interface. The dispersion is nearly linear and the gap is not visible in the figure. (b) Perturbed Wu-Hu interface. An apparent gap is opened with magnitude comparable to the bulk band gap. The pseudospins are mixed showing lighter color. a is the lattice constant.

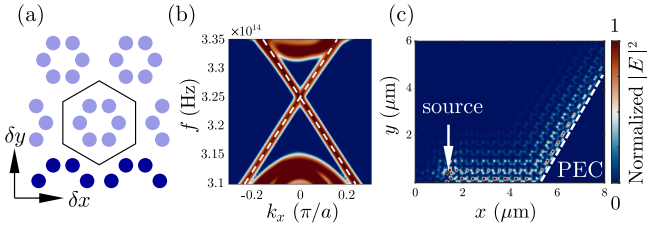

FIG. 4. (a) The schematic of the strip geometry applied for the edge states of a shrunken phase; atoms from bulk complete (edge incomplete) unit cell are colored in light blue (dark blue). The edge is created by cutting through the $1a$ position; then a slight tuning is applied to the incomplete unit cells at the edge. The direction of δx, δy is also noted. (b) Numerically calculated interface dispersion, showing two in-gap linear modes. a is the lattice constant. (c) Large scale simulation of the propagation of a trivial edge state from a circularly polarized source. The open boundary turning is marked in a white dashed line.

preserved. For a system with an interface, we write the perturbed Hamiltonian as

$$H' = H_0 + \Delta H, \tag{4}$$

in which H_0 describes the unperturbed interface of the Wu-Hu model and ΔH is the perturbation. The spectra of interface states for H' and H_0 are shown in Fig. 3. For H_0, there exists a gap at zero energy that is hardly visible (as observed in the Wu-Hu model [16]), whereas for H', the gap is comparable to the bulk band gap. Pseudospin character of the interface states also shows clear mixing for H' compared to H_0, which is consistent with the argument that C_6 symmetry does not imply spin conservation. All these observations strongly suggest that, aside from C_6 symmetry breaking, other mechanisms can open a gap for the interface states, therefore showing the absence of topological protection in the system clearly.

In addition, we compare the Wu-Hu interface and the edge of 2D TIs protected by $\mathcal{T}^2 = -1$ to discuss the relation between their properties and topology. The three properties concerned here are spectral robustness, immunity from backscattering, and spin-momentum locking. For 2D TIs, the spectrally robust edge states can be understood by the topological equivalence between the edge spectrum and the Wilson loop spectrum, which has a stable winding protected by Wannier obstruction [45,46]. The immunity of backscattering is then followed as a combined effect of $\mathcal{T}^2 = -1$ and the presence of odd number of edge states [61]. Lastly, instead of a unique topological phenomenon, the spin-momentum locking is a prevalent feature in edge modes with strong spin-orbit coupling. To conclude, only spectral robustness is directly related to topology, and in bosonic systems with $\mathcal{T}^2 = 1$, the immunity from backscattering cannot be expected. For the Wu-Hu interface, this agrees well with the quantitative experimental results [62].

From a practical perspective, these gapless, backscattering free, and spin-momentum-locked interface states are what make the Wu-Hu model promising for photonic applications. Here, we numerically demonstrate helical edge states that solely stem from the trivial phase of Wu-Hu model with OBCs that reproduce all the features of the claimed "topological" Wu-Hu interface. Structures applied and corresponding bulk band diagrams can be found in the Supplemental Material [52].

We start with the trivial phase of the Wu-Hu model and create edge states by cutting through the Wannier center of the VBs, namely $1a$ Wyckoff position [Fig. 4(a)]. Being of defect nature, the resulted edge states are highly tunable that they can be tuned to be gapless by simply displacing the sites at the edge. We first calculated the dispersion spectrum of a strip geometry of this trivial edge [Figs. 4(a) and 4(b)], with Bloch boundary condition applied in the x direction and OBCs in the y direction (see Supplemental Material [52] for detailed simulation setup including the band dispersion and the eigenmodes at Γ point). Two edge states emerge in the dispersion inside the bulk gap [Fig. 4(b)], showing a dirac-cone-shaped crossing. Then we performed a large scale simulation of the edge states with a sharp bend excited with a circularly polarized source [Fig. 4(c)]. The unidirectional propagation is clearly observed along the sample edge (see Supplemental Material [52] for the demonstration of the unidirectional wave propagating modes), showing that topology is not required for a helical photonic edge.

In conclusion, we re-examined the Wu-Hu model and identified the algebraic nature of the topological invariants and the associated physical consequences. We showed the lack of robustness of its interface states against symmetry preserving perturbations and explicitly constructed a trivial defect edge that reproduces all the "topological" properties. However, the following question remains interesting and unanswered: for TCIs, whether, and to what extent, would Wannier obstructions provide protection to the interface in the domain wall configuration similar to the Wu-Hu model

where the bulk symmetry is partially restored by the addition of a trivial phase? In fact, the existence of such protection is an implicit assumption for the topological interpretation of Wu-Hu interface. If this protection does not exist even when one of the phases is stably obstructed, the topological interpretation of Wu-Hu interface would fail at the first step. Based on our arguments, one cannot distinguish whether the trivial nature of the VBs or the absence of topological protection itself is the fundamental reason that is responsible for the gap opening. The rigorous discussions of similar questions have only appeared recently [47], and we hope our results as a case study can provide some insights to future studies. For photonic waveguide engineering applications, our results show that there is no causal relation between the topology of the Wu-Hu model and the desired properties at its interface. In fact, perfect transmission at sharp bends can be achieved in traditional photonic crystals and spin-momentum locking is a prevalent feature for evanescent electromagnetic waves [63]. The lack of bulk-edge correspondence in the Wu-Hu model enables more flexible designs combining different bulk structures without any symmetry consideration, which may lead to novel applications such as photonic on-chip logic and reconfigurable light routing.

This work was supported by the Office of Naval Research via Grant No. N00014-22-1-2378.

*Corresponding author.
riteshag@seas.upenn.edu
†These authors contributed equally to this work.

[1] S. Raghu and F. D. M. Haldane, Analogs of quantum-Hall-effect edge states in photonic crystals, Phys. Rev. A **78**, 033834 (2008).
[2] F. Haldane and S. Raghu, Possible Realization of Directional Optical Waveguides in Photonic Crystals with Broken Time-Reversal Symmetry, Phys. Rev. Lett. **100**, 013904 (2008).
[3] L. Lu, J. D. Joannopoulos, and M. Soljačić, Topological photonics, Nat. Photonics **8**, 821 (2014).
[4] T. Ozawa, H. M. Price, A. Amo, N. Goldman, M. Hafezi, L. Lu, M. C. Rechtsman, D. Schuster, J. Simon, O. Zilberberg *et al.*, Topological photonics, Rev. Mod. Phys. **91**, 015006 (2019).
[5] X. Zhang, M. Xiao, Y. Cheng, M.-H. Lu, and J. Christensen, Topological sound, Commun. Phys. **1**, 97 (2018).
[6] Z. Wang, Y. D. Chong, J. D. Joannopoulos, and M. Soljačić, Reflection-Free One-Way Edge Modes in a Gyromagnetic Photonic Crystal, Phys. Rev. Lett. **100**, 013905 (2008).
[7] Z. Wang, Y. Chong, J. D. Joannopoulos, and M. Soljačić, Observation of unidirectional backscattering-immune topological electromagnetic states, Nature (London) **461**, 772 (2009).
[8] L. Fu, Topological Crystalline Insulators, Phys. Rev. Lett. **106**, 106802 (2011).
[9] C.-K. Chiu, J. C. Y. Teo, A. P. Schnyder, and S. Ryu, Classification of topological quantum matter with symmetries, Rev. Mod. Phys. **88**, 035005 (2016).
[10] H. C. Po, H. Watanabe, and A. Vishwanath, Fragile Topology and Wannier Obstructions, Phys. Rev. Lett. **121**, 126402 (2018).
[11] Z.-D. Song, L. Elcoro, and B. A. Bernevig, Twisted bulk-boundary correspondence of fragile topology, Science **367**, 794 (2020).
[12] A. Bouhon, A. M. Black-Schaffer, and R.-J. Slager, Wilson loop approach to fragile topology of split elementary band representations and topological crystalline insulators with time-reversal symmetry, Phys. Rev. B **100**, 195135 (2019).
[13] A. Bouhon, T. Bzdušek, and R.-J. Slager, Geometric approach to fragile topology beyond symmetry indicators, Phys. Rev. B **102**, 115135 (2020).
[14] W. A. Benalcazar, B. A. Bernevig, and T. L. Hughes, Quantized electric multipole insulators, Science **357**, 61 (2017).
[15] F. Schindler, A. M. Cook, M. G. Vergniory, Z. Wang, S. S. Parkin, B. A. Bernevig, and T. Neupert, Higher-order topological insulators, Sci. Adv. **4**, eaat0346 (2018).
[16] L.-H. Wu and X. Hu, Scheme for Achieving a Topological Photonic Crystal by Using Dielectric Material, Phys. Rev. Lett. **114**, 223901 (2015).
[17] S. Barik, A. Karasahin, C. Flower, T. Cai, H. Miyake, W. DeGottardi, M. Hafezi, and E. Waks, A topological quantum optics interface, Science **359**, 666 (2018).
[18] Y. Yang, Y. F. Xu, T. Xu, H.-X. Wang, J.-H. Jiang, X. Hu, and Z. H. Hang, Visualization of a Unidirectional Electromagnetic Waveguide Using Topological Photonic Crystals Made of Dielectric Materials, Phys. Rev. Lett. **120**, 217401 (2018).
[19] D. Smirnova, S. Kruk, D. Leykam, E. Melik-Gaykazyan, D.-Y. Choi, and Y. Kivshar, Third-Harmonic Generation in Photonic Topological Metasurfaces, Phys. Rev. Lett. **123**, 103901 (2019).
[20] Z.-K. Shao, H.-Z. Chen, S. Wang, X.-R. Mao, Z.-Q. Yang, S.-L. Wang, X.-X. Wang, X. Hu, and R.-M. Ma, A high-performance topological bulk laser based on band-inversion-induced reflection, Nat. Nanotechnol. **15**, 67 (2020).
[21] A. Dikopoltsev, T. H. Harder, E. Lustig, O. A. Egorov, J. Beierlein, A. Wolf, Y. Lumer, M. Emmerling, C. Schneider, S. Höfling *et al.*, Topological insulator vertical-cavity laser array, Science **373**, 1514 (2021).
[22] W. Liu, M. Hwang, Z. Ji, Y. Wang, G. Modi, and R. Agarwal, z_2 photonic topological insulators in the visible wavelength range for robust nanoscale photonics, Nano Lett. **20**, 1329 (2020).
[23] W. Liu, Z. Ji, Y. Wang, G. Modi, M. Hwang, B. Zheng, V. J. Sorger, A. Pan, and R. Agarwal, Generation of helical topological exciton-polaritons, Science **370**, 600 (2020).
[24] A. Kumar, M. Gupta, P. Pitchappa, N. Wang, M. Fujita, and R. Singh, Terahertz topological photonic integrated circuits for 6g and beyond: A perspective, J. Appl. Phys. **132**, 140901 (2022).
[25] Z. Zhang, Q. Wei, Y. Cheng, T. Zhang, D. Wu, and X. Liu, Topological Creation of Acoustic Pseudospin Multipoles in a Flow-Free Symmetry-Broken Metamaterial Lattice, Phys. Rev. Lett. **118**, 084303 (2017).

[26] Z.-Q. Yang, Z.-K. Shao, H.-Z. Chen, X.-R. Mao, and R.-M. Ma, Spin-Momentum-Locked Edge Mode for Topological Vortex Lasing, Phys. Rev. Lett. **125**, 013903 (2020).

[27] Y. Liu, C.-S. Lian, Y. Li, Y. Xu, and W. Duan, Pseudospins and Topological Effects of Phonons in a Kekulé Lattice, Phys. Rev. Lett. **119**, 255901 (2017).

[28] H. Pirie, S. Sadhuka, J. Wang, R. Andrei, and J. E. Hoffman, Topological Phononic Logic, Phys. Rev. Lett. **128**, 015501 (2022).

[29] J. Cha, K. W. Kim, and C. Daraio, Experimental realization of on-chip topological nanoelectromechanical metamaterials, Nature (London) **564**, 229 (2018).

[30] C. He, X. Ni, H. Ge, X.-C. Sun, Y.-B. Chen, M.-H. Lu, X.-P. Liu, and Y.-F. Chen, Acoustic topological insulator and robust one-way sound transport, Nat. Phys. **12**, 1124 (2016).

[31] M. Li, I. Sinev, F. Benimetskiy, T. Ivanova, E. Khestanova, S. Kiriushechkina, A. Vakulenko, S. Guddala, M. Skolnick, V. M. Menon *et al.*, Experimental observation of topological z_2 exciton-polaritons in transition metal dichalcogenide monolayers, Nat. Commun. **12**, 4425 (2021).

[32] S. Barik, H. Miyake, W. DeGottardi, E. Waks, and M. Hafezi, Two-dimensionally confined topological edge states in photonic crystals, New J. Phys. **18**, 113013 (2016).

[33] M. B. de Paz, M. G. Vergniory, D. Bercioux, A. García-Etxarri, and B. Bradlyn, Engineering fragile topology in photonic crystals: Topological quantum chemistry of light, Phys. Rev. Res. **1**, 032005(R) (2019).

[34] S. J. Palmer and V. Giannini, Berry bands and pseudo-spin of topological photonic phases, Phys. Rev. Res. **3**, L022013 (2021).

[35] M. Proctor, P. A. Huidobro, B. Bradlyn, M. B. de Paz, M. G. Vergniory, D. Bercioux, and A. García-Etxarri, Robustness of topological corner modes in photonic crystals, Phys. Rev. Res. **2**, 042038(R) (2020).

[36] M. B. de Paz, M. Herrera, P. A. Huidobro, H. Alaeian, M. Vergniory, B. Bradlyn, G. Giedke, A. García-Etxarri, and D. Bercioux, Energy density as a probe of band representations in photonic crystals, J. Phys. Condens. Matter **34**, 314002 (2022).

[37] J. Noh, W. A. Benalcazar, S. Huang, M. J. Collins, K. P. Chen, T. L. Hughes, and M. C. Rechtsman, Topological protection of photonic mid-gap defect modes, Nat. Photonics **12**, 408 (2018).

[38] J. Zak, Band representations of space groups, Phys. Rev. B **26**, 3010 (1982).

[39] L. Michel and J. Zak, Elementary energy bands in crystals are connected, Phys. Rep. **341**, 377 (2001).

[40] J. Cano, B. Bradlyn, Z. Wang, L. Elcoro, M. G. Vergniory, C. Felser, M. I. Aroyo, and B. A. Bernevig, Building blocks of topological quantum chemistry: Elementary band representations, Phys. Rev. B **97**, 035139 (2018).

[41] R.-J. Slager, A. Mesaros, V. Juričić, and J. Zaanen, The space group classification of topological band-insulators, Nat. Phys. **9**, 98 (2013).

[42] J. Kruthoff, J. de Boer, J. van Wezel, C. L. Kane, and R.-J. Slager, Topological Classification of Crystalline Insulators through Band Structure Combinatorics, Phys. Rev. X **7**, 041069 (2017).

[43] A. Alexandradinata, X. Dai, and B. A. Bernevig, Wilson-loop characterization of inversion-symmetric topological insulators, Phys. Rev. B **89**, 155114 (2014).

[44] B. Bradlyn, Z. Wang, J. Cano, and B. A. Bernevig, Disconnected elementary band representations, fragile topology, and Wilson loops as topological indices: An example on the triangular lattice, Phys. Rev. B **99**, 045140 (2019).

[45] A. Alexandradinata, Z. Wang, and B. A. Bernevig, Topological Insulators from Group Cohomology, Phys. Rev. X **6**, 021008 (2016).

[46] L. Fidkowski, T. S. Jackson, and I. Klich, Model Characterization of Gapless Edge Modes of Topological Insulators Using Intermediate Brillouin Zone Functions, Phys. Rev. Lett. **107**, 036601 (2011).

[47] A. Alexandradinata, J. Höller, C. Wang, H. Cheng, and L. Lu, Crystallographic splitting theorem for band representations and fragile topological photonic crystals, Phys. Rev. B **102**, 115117 (2020).

[48] B. Bradlyn, L. Elcoro, J. Cano, M. G. Vergniory, Z. Wang, C. Felser, M. I. Aroyo, and B. A. Bernevig, Topological quantum chemistry, Nature (London) **547**, 298 (2017).

[49] M. I. Aroyo, J. M. Perez-Mato, C. Capillas, E. Kroumova, S. Ivantchev, G. Madariaga, A. Kirov, and H. Wondratschek, Bilbao crystallographic server: I. Databases and crystallographic computing programs, Z. Kristallogr.-Cryst. Mater. **221**, 15 (2006).

[50] M. I. Aroyo, A. Kirov, C. Capillas, J. Perez-Mato, and H. Wondratschek, Bilbao crystallographic server. II. Representations of crystallographic point groups and space groups, Acta Crystallogr. Sect. A **62**, 115 (2006).

[51] M. I. Aroyo, J. M. Perez-Mato, D. Orobengoa, E. Tasci, G. de la Flor, and A. Kirov, Crystallography online: Bilbao crystallographic server, Bulg. Chem. Commun. **43**, 183 (2011), http://bcc.bas.bg/BCC_Volumes/Volume_43_Number_2_2011/Volume_43_Number_2_2011_PDF/2011_43_2_1.pdf.

[52] See Supplemental Material at http://link.aps.org/supplemental/10.1103/PhysRevLett.131.053802 for the discussion of the topological invariants of the model, the detailed setup of the perturbed Hamiltonian, and numerical simulations of trivial helical edge states, including the band dispersion and the eigenmodes at Γ point showing the band inversion, the demonstration of the dependence of the edge parameters of the edge state dispersion, and its unidirectional propagating, which includes Ref. [53].

[53] F. Liu, H.-Y. Deng, and K. Wakabayashi, Helical Topological Edge States in a Quadrupole Phase, Phys. Rev. Lett. **122**, 086804 (2019).

[54] J. Ahn, S. Park, D. Kim, Y. Kim, and B.-J. Yang, Stiefel–whitney classes and topological phases in band theory, Chin. Phys. B **28**, 117101 (2019).

[55] A. Bouhon, Q. Wu, R.-J. Slager, H. Weng, O. V. Yazyev, and T. Bzdušek, Non-Abelian reciprocal braiding of Weyl points and its manifestation in ZrTe, Nat. Phys. **16**, 1137 (2020).

[56] B. Jiang, A. Bouhon, Z.-K. Lin, X. Zhou, B. Hou, F. Li, R.-J. Slager, and J.-H. Jiang, Experimental observation of non-Abelian topological acoustic semimetals and their phase transitions, Nat. Phys. **17**, 1239 (2021).

[57] B. Peng, A. Bouhon, B. Monserrat, and R.-J. Slager, Phonons as a platform for non-Abelian braiding and its manifestation in layered silicates, Nat. Commun. **13**, 423 (2022).

[58] B. J. Wieder and B. A. Bernevig, The axion insulator as a pump of fragile topology, arXiv:1810.02373.

[59] Z. Wang, B. J. Wieder, J. Li, B. Yan, and B. A. Bernevig, Higher-Order Topology, Monopole Nodal Lines, and the Origin of Large Fermi Arcs in Transition Metal Dichalcogenides $X\mathrm{Te}_2$ (x = Mo, W), Phys. Rev. Lett. **123**, 186401 (2019).

[60] J. Ahn, S. Park, and B.-J. Yang, Failure of Nielsen-Ninomiya Theorem and Fragile Topology in Two-Dimensional Systems with Space-Time Inversion Symmetry: Application to Twisted Bilayer Graphene at Magic Angle, Phys. Rev. X **9**, 021013 (2019).

[61] C. L. Kane and E. J. Mele, Quantum Spin Hall Effect in Graphene, Phys. Rev. Lett. **95**, 226801 (2005).

[62] B. Orazbayev and R. Fleury, Quantitative robustness analysis of topological edge modes in c6 and valley-Hall metamaterial waveguides, Nanophotonics **8**, 1433 (2019).

[63] T. Van Mechelen and Z. Jacob, Universal spin-momentum locking of evanescent waves, Optica **3**, 118 (2016).